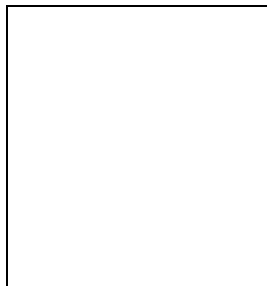


Determination of ϕ_2 (α) and ϕ_3 (γ)

Akito Kusaka

*Department of Physics, University of Tokyo,
7-3-1, Hongo, Bunkyo-ku, 113-0033 Tokyo, Japan*



We review recent measurements constraining the Cabibbo-Kobayashi-Maskawa weak phases ϕ_2 (α) and ϕ_3 (γ) at two energy-asymmetric B -factories, Belle/KEKB and BaBar/PEP-II. The measurements of decay processes $B \rightarrow \pi\pi$, $\rho\rho$, and $\rho\pi$ yield dominant constraint on ϕ_2 . The recent measurement of the process $B \rightarrow a_1\pi$ is also sensitive to ϕ_2 . The phase ϕ_3 is mainly measured using the decay process of $B^+ \rightarrow D^{(*)}K^+$.

1 Introduction

CP violation arises from irreducible phase in Cabibbo-Kobayashi-Maskawa (CKM) matrix,^{1,2} which is established as a part of the standard model (SM) by various experimental observations, in particular those from the asymmetric energy B -factories.^{3,4} Now, we have entered a new era of the physics of CP violation; we use it as a probe sensitive to the physics beyond the SM, or new physics. To examine whether all the observables are universally described by the CKM picture is a quest for the new physics, since we expect to see deviations from the CKM expectations if there contributes the new physics effect.

The test of the unitarity of the CKM matrix, $V_{ud}V_{ub}^* + V_{cd}V_{cb}^* + V_{td}V_{tb}^* = 0$, is one of the most important new physics searches in this sense. The angles ϕ_2 and ϕ_3 ^a denotes the CP -violating weak phases $\arg[-V_{td}V_{tb}^*/V_{ud}V_{ub}^*]$ and $\arg[-V_{ud}V_{ub}^*/V_{cd}V_{cb}^*]$, respectively, and their measurements are crucial for the test of the unitarity.

In this proceedings, we present the review of recent measurements of the angles ϕ_2 and ϕ_3 at Belle/KEKB and BaBar/PEP-II.

^aAnother naming convention, $\alpha(= \phi_2)$ and $\gamma(= \phi_3)$, are also used in the literature.

2 Determination of ϕ_2 (α)

The angle ϕ_2 is the complex phase of $-V_{td}V_{tb}^*/V_{ud}V_{ub}^*$ and we can access it via the decay processes that involve those CKM factors. As shown in Fig. 1, the factor $V_{td}V_{tb}^*$ arises from B^0 - \bar{B}^0 mixing and $V_{ud}V_{ub}^*$ appears in the decay processes that involve $b \rightarrow u$ transition, such as $B^0 \rightarrow \pi^+\pi^-$, $\rho^+\rho^-$, $\rho^\pm\pi^\mp$, and $a_1^\pm\pi^\mp$; we can constrain ϕ_2 by the measurements of these processes.

In the decay chain $\Upsilon(4S) \rightarrow B^0\bar{B}^0 \rightarrow ff_{\text{tag}}$, where f is the final states of interest (e.g., $\pi^+\pi^-$, $\rho^+\rho^-$, $\rho^\pm\pi^\mp$, and $a_1^\pm\pi^\mp$) and f_{tag} is a final state that distinguishes B^0 and \bar{B}^0 , the time-dependent differential decay rate is^{5,6,7}

$$\frac{d\Gamma}{d\Delta t} \propto e^{-|\Delta t|/\tau_{B^0}} \left[1 + q_{\text{tag}} \{ \mathcal{A}_f \cos(\Delta m_d \Delta t) + \mathcal{S}_f \sin(\Delta m_d \Delta t) \} \right]. \quad (1)$$

Here, q_{tag} is the b -flavor charge [$q_{\text{tag}} = +1(-1)$ when f_{tag} is a B^0 (\bar{B}^0) flavor eigenstate], Δt is the decay time difference between the two B mesons ($t_f - t_{f_{\text{tag}}}$), and τ_{B^0} and Δm_d are the average lifetime and mass difference of the mass eigenstates of neutral B mesons, respectively. The CP -violation parameters \mathcal{A}_f and \mathcal{S}_f are the observables of the measurement. In a decay process of $b \rightarrow u$ transition, \mathcal{S}_f is related to ϕ_2 as

$$\mathcal{S}_f = \sin 2\phi_2, \quad (2)$$

ignoring the penguin diagram contribution described in the followings.

The difficulty in the measurement of ϕ_2 through the decays with $b \rightarrow u$ transition arises out of the possible contribution from the gluonic penguin diagram of $b \rightarrow d$ transition (Fig. 2). This contribution contaminates the measurement of ϕ_2 , since the decays via this diagram yields the CKM factor $V_{td}V_{tb}^*$, which is different from that of the $b \rightarrow u$ transition. With the contamination, Eq. (2) becomes

$$\mathcal{S}_f = \sqrt{1 - \mathcal{A}_f^2} \sin 2\phi_2^{\text{eff},f}, \quad (3)$$

where $\phi_2^{\text{eff},f}$ may differ from ϕ_2 . Large amount of effort (both experimental and theoretical) is devoted to constrain the difference between $\phi_2^{\text{eff},f}$ and ϕ_2 , as well as the measurement of the CP -violation parameters \mathcal{A}_f and \mathcal{S}_f .

The isospin analysis⁸ gives constraint on the difference $|\phi_2^{\text{eff},f} - \phi_2|$ by incorporating the knowledge of processes related the modes. In the case of $B \rightarrow \pi\pi$, for example, it involves the decay modes $B^0 \rightarrow \pi^0\pi^0$ and $B^+ \rightarrow \pi^+\pi^0$ in addition to $B^0 \rightarrow \pi^+\pi^-$; one can constrain $|\phi_2^{\text{eff},\pi\pi} - \phi_2|$ by the measurements of branching fractions and CP asymmetries of these modes. There are several methods other than the isospin analysis for the removal of the penguin diagram contamination. One is the time-dependent Dalitz plot analysis in $B^0 \rightarrow (\rho\pi)^0 \rightarrow \pi^+\pi^-\pi^0$ decay process,⁹ which is used along with an isospin relation.^{10,11} Another is the use of theoretical assumptions,^{12,13,14,15} such as the flavor $SU(3)$ symmetry; it enables us to relate the CP -violation measurement of $B^0 \rightarrow a_1^\pm\pi^\mp$ to ϕ_2 , as well as the decay modes of $B^0 \rightarrow \pi^+\pi^-$, $\rho^+\rho^-$, and $\rho^\pm\pi^\mp$.

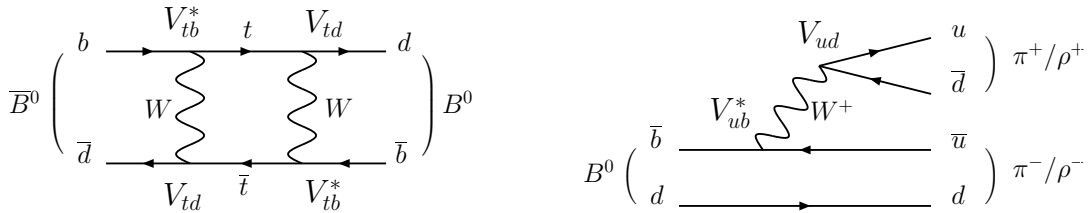


Figure 1: Feynman diagrams corresponding to the B^0 - \bar{B}^0 mixing (left) and the B^0 decay via $b \rightarrow u$ transition (right).

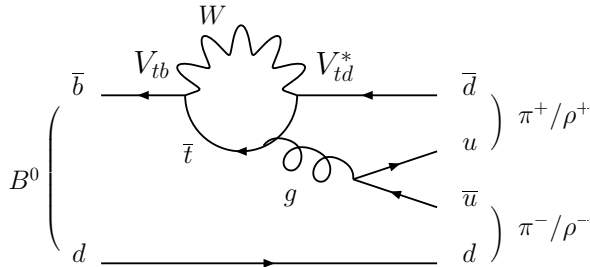


Figure 2: Gluonic penguin diagram of the B^0 decay via $b \rightarrow d$ transition.

2.1 $B \rightarrow \pi\pi$

Belle and BaBar measure the CP violation in the decay process $B^0 \rightarrow \pi^+\pi^-$ with data samples containing 535×10^6 and 383×10^6 $B\bar{B}$ pairs, respectively.^{16,17} Table 1 lists the results. Belle reports the first observation of the direct CP violation ($\mathcal{A}_{\pi^+\pi^-} \neq 0$) with a significance of 5.5 standard deviations (σ). BaBar observes CP violation ($\mathcal{C}_{\pi^+\pi^-} \neq 0$ and $\mathcal{S}_{\pi^+\pi^-} \neq 0$) with a significance of 5.4σ , though it does not see significant direct CP violation. The discrepancy between the results from Belle and BaBar corresponds to the significance of 2.1σ . From the above result and world averaged values for $\mathcal{B}(B^0 \rightarrow \pi^+\pi^-)$, $\mathcal{B}(B^0 \rightarrow \pi^0\pi^0)$, $\mathcal{B}(B^+ \rightarrow \pi^+\pi^0)$, and $\mathcal{A}(B^0 \rightarrow \pi^0\pi^0)$,¹⁸ Belle constrain ϕ_2 and excludes the region $11^\circ < \phi_2 < 79^\circ$ at the 95% confidence level (C.L.). Further discussion on the ϕ_2 constraint using the above mentioned results can be found elsewhere.^{19,20}

Table 1: The results of the latest measurements of CP violation in the decay $B^0 \rightarrow \pi^+\pi^-$ at Belle and BaBar. The first and second errors are statistical and systematic, respectively. Note that they use different conventions for the coefficient of $\cos(\Delta m_d \Delta t)$, $\mathcal{A}_{\pi^+\pi^-}$ and $\mathcal{C}_{\pi^+\pi^-}$, which are equivalent except for the opposite sign.

	$\mathcal{A}_{\pi^+\pi^-} (= -\mathcal{C}_{\pi^+\pi^-})$	$\mathcal{S}_{\pi^+\pi^-}$
Belle ¹⁶	$+0.55 \pm 0.08 \pm 0.05$	$-0.61 \pm 0.10 \pm 0.04$
BaBar ¹⁷	$+0.21 \pm 0.09 \pm 0.02$	$-0.60 \pm 0.11 \pm 0.03$

2.2 $B \rightarrow \rho\rho$

There are two essential differences between $B \rightarrow \rho\rho$ and $B \rightarrow \pi\pi$: 1) ρ is a vector meson, while π is a pseudo-scalar meson, and 2) the contribution from the $b \rightarrow d$ penguin diagram is small in $B \rightarrow \rho\rho$ than in $B \rightarrow \pi\pi$. In principle, the first difference is a disadvantage of $B \rightarrow \rho\rho$, since it leads to the fact that the final state is a mixture of three polarization states with different CP eigenvalues. In practice, however, it is not because one of the polarization state, the longitudinal polarization, turned out to dominate the final state in all of the processes of $B^0 \rightarrow \rho^+\rho^-$, $\rho^0\rho^0$, and $B^+ \rightarrow \rho^+\rho^0$ ^{21,22,23,24,25}; this enables us to relate the measurements to ϕ_2 without the effort to disentangle a single polarization state. The second difference, the smallness of the penguin diagram contribution, is deduced by the smallness of the branching fraction of $B^0 \rightarrow \rho^0\rho^0$ ²³, compared to those of $B^0 \rightarrow \rho^+\rho^-$ and $B^+ \rightarrow \rho^+\rho^0$. The smaller penguin leads to the smaller $|\phi_2^{\text{eff},\rho\rho} - \phi_2|$ and thus the better constraint on ϕ_2 .

Table 2 lists the latest measurements of the CP violation in the process $B^0 \rightarrow \rho^+\rho^-$ at Belle and BaBar using data samples containing 535×10^6 and 347×10^6 $B\bar{B}$ pairs, respectively. The results are consistent with $\mathcal{S}_{\rho^+\rho^-} = 0$, which correspond to $\phi_2 \sim 90^\circ$ at the limit of no penguin contribution. A drastic change in the ϕ_2 constraint came from the new measurements of the branching fractions of $B^0 \rightarrow \rho^0\rho^0$ and $B^+ \rightarrow \rho^+\rho^0$ ^{25,23} (Table 3) Before the new measurements,

the isospin triangles were in squashed shapes due to the small branching fractions of $B^0 \rightarrow \rho^+ \rho^-$ and $\rho^0 \rho^0$ compared to $B^+ \rightarrow \rho^+ \rho^0$, leading to the good constraint on $|\phi_2 - \phi_2^{\text{eff}}|$; with the new measurements, the triangles are now normally shaped and the constraint gets modest. For further improvement of the ϕ_2 constraint, we have to measure the CP asymmetry of $B^0 \rightarrow \rho^0 \rho^0$ decay process or to assume some theoretical input such as flavor $SU(3)$.

From the above mentioned measurements, Belle obtains the constraint of $54^\circ < \phi_2 < 113^\circ$ at the 90% C.L., while BaBar obtains $\phi_2^{\text{eff}} = (95.5_{-6.2}^{+6.9})^\circ$ and $|\phi_2 - \phi_2^{\text{eff}}| < 18^\circ$ at 68% C.L. Further discussion can be found elsewhere.^{19,20}

Table 2: The latest measurements of the CP violation, polarization, and branching fraction of the decay $B^0 \rightarrow \rho^+ \rho^-$ at Belle and BaBar. The first and second errors are statistical and systematic, respectively. Note that the branching fraction and polarization measurements at Belle uses a different data sample from that used for the

CP violation measurement.				
	$\mathcal{A}_{\rho^+ \rho^-} (= -\mathcal{C}_{\rho^+ \rho^-})$	$\mathcal{S}_{\rho^+ \rho^-}$	$\mathcal{B} (\times 10^{-6})$	f_L
Belle ^{21,26}	$+0.16 \pm 0.21 \pm 0.07$	$+0.19 \pm 0.30 \pm 0.07$	$22.8 \pm 3.8_{-2.6}^{+2.3}$	$0.941_{-0.040}^{+0.034} \pm 0.030$
BaBar ²²	$+0.07 \pm 0.15 \pm 0.06$	$-0.19 \pm 0.21_{-0.07}^{+0.05}$	$23.5 \pm 2.2 \pm 4.1$	$0.977 \pm 0.024_{-0.013}^{+0.015}$

Table 3: The latest measurements of the branching fractions and longitudinal fractions of the decays $B^0 \rightarrow \rho^0 \rho^0$ and $B^+ \rightarrow \rho^+ \rho^0$. The first and second errors are statistical and systematic, respectively.

	$B^+ \rightarrow \rho^+ \rho^0$		$B^0 \rightarrow \rho^0 \rho^0$	
	$\mathcal{B} (\times 10^{-6})$	f_L	$\mathcal{B} (\times 10^{-6})$	f_L
Belle ²⁴	$31.7 \pm 7.1_{-6.7}^{+3.8}$	$0.948 \pm 0.106 \pm 0.021$	—	—
BaBar ^{25,23}	$16.8 \pm 2.2 \pm 2.3$	$0.905 \pm 0.042_{-0.027}^{+0.023}$	$1.07 \pm 0.33 \pm 0.19$	$0.87 \pm 0.13 \pm 0.04$

2.3 $B \rightarrow \rho \pi$

The time-dependent Dalitz plot analysis of the decay $B^0 \rightarrow \rho \pi \rightarrow \pi^+ \pi^- \pi^0$ offers a unique way to determine the angle ϕ_2 ; in contrast to the other analyses, it includes measurement of CP -violating asymmetries in mixed final states. In the limit of high statistics, this enables us to obtain ϕ_2 without discrete ambiguities.

Belle and BaBar have recently released the complete time-dependent Dalitz plot analysis of the $B^0 \rightarrow \pi^+ \pi^- \pi^0$ decay process for the first time using data samples corresponding to 449×10^6 and 375×10^6 $B\bar{B}$ pairs, respectively.^{27,28} From the result, BaBar obtains the constraint $\phi_2 = (87_{-13}^{+45})^\circ$ at 68% C.L. Belle performs a combined analysis of the time-dependent Dalitz plot and isospin (pentagon) analysis and obtains $68^\circ < \phi_2 < 95^\circ$ as a 68% confidence interval consistent with the SM, though a large SM-disfavored region also remains. BaBar have also released the new measurement of the branching fraction ($[10.2 \pm 1.4(\text{stat}) \pm 0.9(\text{syst})] \times 10^{-6}$) and CP asymmetry ($\mathcal{A} = -0.01 \pm 0.13(\text{stat}) \pm 0.02(\text{syst})$) in the decay $B^+ \rightarrow \rho^+ \pi^0$,²⁹ which can be used to improve the ϕ_2 constraint from the pentagon analysis.

2.4 $B \rightarrow a_1 \pi$

The process $B^0 \rightarrow a_1^\pm \pi^\mp$ is also described by the diagrams of Figs. 1 and 2 and one can obtain information on ϕ_2 through the time-dependent CP violation measurement of this process, though the final states $a_1^\pm \pi^\mp$ are not CP eigenstates. BaBar reports the measurement using a data sample containing 384×10^6 $B\bar{B}$ pairs, obtaining $\phi_2^{\text{eff}} = 78.6^\circ \pm 7.3^\circ$, where the error includes both statistical and systematic errors.³⁰ Since the isospin analysis is difficult to perform with this

process, one basically have to rely on theoretical assumption such as flavor $SU(3)$ ¹⁴ to extract ϕ_2 from the experimentally measured ϕ_2^{eff} .

3 Determination of ϕ_3 (γ)

The angle ϕ_3 is the complex phase of $-V_{ud}V_{ub}^*/V_{cd}V_{cb}^*$. As shown in Fig. 3, the factors V_{cb}^* and V_{us} ($\sim V_{cd}$) appears in the process of $B^- \rightarrow D^{(*)0}K^-$ decay, while the process $B^- \rightarrow \bar{D}^{(*)0}K^-$ involves the factors V_{ub}^* and V_{cs} ($\sim V_{ud}$). Thus, one can access ϕ_3 via a decay process of $B^- \rightarrow fK^-$ where f is a final state to which both $D^{(*)0}$ and $\bar{D}^{(*)0}$ can decay.

The decay amplitudes of the processes $B^+ \rightarrow DK^+(D \rightarrow \bar{f})$ and $B^- \rightarrow DK^-(D \rightarrow f)$ are written as

$$\begin{aligned} A(B^+ \rightarrow DK^+) &\propto A_D + r_B e^{+i\phi_3+i\delta} A_{\bar{D}}, \\ A(B^- \rightarrow DK^-) &\propto A_D + r_B e^{-i\phi_3+i\delta} A_{\bar{D}}, \end{aligned} \quad (4)$$

where A_D and $A_{\bar{D}}$ are the decay amplitudes of $D^{(*)0} \rightarrow f$ and $\bar{D}^{(*)0} \rightarrow f$, respectively^b; $r_B = |A(B^- \rightarrow \bar{D}^{(*)0}K^-)|/|A(B^- \rightarrow D^{(*)0}K^-)|$; and δ is the strong phase difference between $B^- \rightarrow \bar{D}^{(*)0}K^-$ and $B^- \rightarrow D^{(*)0}K^-$. As can be seen in the equations, the dependence on ϕ_3 can manifest itself as the interference between the first and second terms in the right hand side; the comparison of the interference effects in B^+ and B^- decays is sensitive to ϕ_3 . The difficulty in using this decay process comes from the smallness of r_B (~ 0.1), which is mainly due to color suppression. The methods of the analysis can be categorized into the following three by the types of the final state f : Dalitz plot,^{31,32} GLW (Gronau-London-Wyler),^{33,34} and ADS (Atwood-Dunietz-Soni).^{35,36}

Another possibility to access ϕ_3 is the time dependent CP violation measurement of $B^0 \rightarrow D^{(*)\pm}\pi^\mp$ decay process, which is sensitive to $\sin(2\phi_1 + \phi_3)$.^{37,38} Since ϕ_1 is very well measured compared to ϕ_3 , it is virtually a measurement of ϕ_3 .

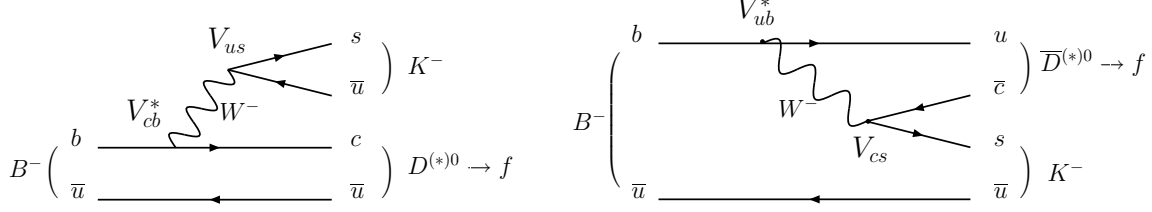


Figure 3: Feynman diagrams corresponding to the $B^- \rightarrow D^{(*)0}K^-$ decay (left) and $B^- \rightarrow \bar{D}^{(*)0}K^-$ (right).

3.1 Dalitz Plot Analysis

In the Dalitz plot analysis, one chooses the three body final state of $K_S\pi^+\pi^-$ as the common final state of f and \bar{f} . In this case, the D decay amplitudes of A_D and $A_{\bar{D}}$ have Dalitz plot dependence as

$$A_D = f(m_-^2, m_+^2) \quad \text{and} \quad A_{\bar{D}} = f(m_+^2, m_-^2), \quad (5)$$

where m_- and m_+ are the invariant mass of $K_S\pi^+$ and $K_S\pi^-$, respectively; and $f(m_+^2, m_-^2)$ is the complex Dalitz plot amplitude of $\bar{D}^0 \rightarrow K_S\pi^+\pi^-$ decay, which is well calibrated using large data samples of $e^+e^- \rightarrow c\bar{c}$ events.

^bHere, no CP violation in D decays is assumed, i.e., we assume

$$A(D^{(*)0} \rightarrow f) = A(\bar{D}^{(*)0} \rightarrow \bar{f}) \quad \text{and} \quad A(\bar{D}^{(*)0} \rightarrow f) = A(D^{(*)0} \rightarrow \bar{f}).$$

Both Belle and BaBar obtain the constraint on ϕ_3 using this method.^{39,40} Belle analyzes the decays of $B^+ \rightarrow DK^+$, D^*K^+ , and DK^{*+} using a data sample containing $388 \times 10^6 B\bar{B}$ pairs and obtains $\phi_3 = (53_{-18}^{+15}[\text{stat}] \pm 3[\text{syst}] \pm 9[\text{model}])^\circ$, while BaBar obtains $\phi_3 = (92 \pm 41[\text{stat}] \pm 11[\text{syst}] \pm 12[\text{model}])^\circ$ based on an analysis of the decays of $B^+ \rightarrow DK^+$ and D^*K^+ using a data sample containing $347 \times 10^6 B\bar{B}$ pairs. Note that the significant difference of the statistical errors between Belle and BaBar is due to their central values of r_B ; BaBar happens to obtain smaller r_B than Belle, leading to the less sensitivity to ϕ_3 . BaBar has recently shown another possibility of using the decay of $D \rightarrow \pi^+\pi^-\pi^0$ for the Dalitz plot analysis.⁴¹

3.2 GLW

In GLW, CP eigenstates are chosen as the common final state f . With CP -even (K^+K^- , $\pi^+\pi^-$) and CP -odd ($K_S\pi^0$, $K_S\omega$, $K_S\phi$, etc.) eigenstates denoted by D_+ and D_- , the direct CP -violating asymmetry \mathcal{A}_\pm is calculated from Eq. (4) as

$$\mathcal{A}_\pm = \frac{\mathcal{B}(B^- \rightarrow D_\pm K^-) - \mathcal{B}(B^+ \rightarrow D_\pm K^+)}{\mathcal{B}(B^- \rightarrow D_\pm K^-) + \mathcal{B}(B^+ \rightarrow D_\pm K^+)} = \frac{\pm r_B \sin \delta \sin \phi_3}{1 + r_B^2 \pm 2r_B \sin \delta \sin \phi_3}. \quad (6)$$

These are sensitive to ϕ_3 combined with the additional information from double ratio of the branching fractions

$$\mathcal{R}_\pm = \frac{\mathcal{B}(B \rightarrow D_\pm K)/\mathcal{B}(B \rightarrow D_\pm \pi)}{\mathcal{B}(B \rightarrow D^0 K)/\mathcal{B}(B \rightarrow D^0 \pi)} = 1 + r_B^2 \pm 2r_B \sin \delta \sin \phi_3. \quad (7)$$

Note that one has to observe significant direct CP violation to constrain ϕ_3 using this method alone.

Belle and BaBar report the measurements with this method using data samples containing 275×10^6 and $232 \times 10^6 B\bar{B}$ pairs, respectively.^{42,43,44} Though neither of the experiments observe significant direct CP violation, the information is still useful in the global fit to constrain ϕ_3 .

3.3 ADS

The ADS method uses the Cabibbo suppressed mode, such as $D^0 \rightarrow K^+\pi^-$, for the final state f . By this choice, the two decay processes of $B^- \rightarrow D^0 K^-$ ($D^0 \rightarrow K^+\pi^-$) and $B^- \rightarrow \bar{D}^0 K^-$ ($\bar{D}^0 \rightarrow K^+\pi^-$) have comparably small branching fractions; the former is Cabibbo suppressed and the latter is color suppressed. The ratio of the branching fractions between the favored and suppressed decay processes is sensitive to ϕ_3 as

$$\mathcal{R}_{DK} = \frac{B^- \rightarrow D(\rightarrow K^+\pi^-)K^-}{B^- \rightarrow D(\rightarrow K^-\pi^+)K^-} = r_B^2 + r_D^2 + 2r_B r_D \cos \phi_3 \cos \delta, \quad (8)$$

where r_D is the Cabibbo suppression factor defined as $r_D = |A(D^0 \rightarrow K^+\pi^-)|/|A(\bar{D}^0 \rightarrow K^+\pi^-)|$. The advantage of this method is that the interference effect is significant with the two interfering decay processes having the similar branching fractions. The disadvantage is, on the other hand, the smallness of the branching fraction of the suppressed decay process, leading to large statistical uncertainty.

Belle and BaBar perform the analysis using data samples containing 275×10^6 and $232 \times 10^6 B\bar{B}$ pairs, respectively; neither of them see significant signal for the suppressed decay processes.^{45,46} They obtain the constraint on r_B based on the upper limit on the branching fractions of the suppressed decays: at 90% C.L., Belle constrain $r_B < 0.18$ for the decay process of $B \rightarrow DK$, while BaBar constrain $r_B < 0.23$ ($r_B < 0.16$) for the $B \rightarrow DK$ ($B \rightarrow D^*K$) decay process. This knowledge can be used in the global fit to constrain ϕ_3 .

3.4 Time-Dependent Analysis of $B^0 \rightarrow D^{(*)\pm}\pi^\mp$ for $\sin(2\phi_1 + \phi_3)$

The time-dependent decay rates of the $B^0 \rightarrow D^{(*)\pm}\pi^\mp$ decay processes are given by⁴⁷

$$P(B^0 \rightarrow D^{(*)\pm}\pi^\mp) \propto e^{-|\Delta t|/\tau_{B^0}} \left[1 \mp C \cos(\Delta m_d \Delta t) - S^\pm \sin(\Delta m_d \Delta t) \right], \quad (9)$$

$$P(\bar{B}^0 \rightarrow D^{(*)\pm}\pi^\mp) \propto e^{-|\Delta t|/\tau_{B^0}} \left[1 \pm C \cos(\Delta m_d \Delta t) + S^\pm \sin(\Delta m_d \Delta t) \right], \quad (10)$$

where C and S^\pm are the observables in the measurement. They can be related to $\sin(2\phi_1 + \phi_3)$ as

$$S^\pm = \frac{2(-1)^L R \sin(2\phi_1 + \phi_3 \pm \delta)}{1 + R^2} \quad \left(R^2 = \frac{1 - C}{1 + C} \right), \quad (11)$$

where L is the angular momentum of the final state.

Belle and BaBar perform the time-dependent analysis using data samples containing 386×10^6 and 232×10^6 $B\bar{B}$ pairs, respectively.^{48,49,50} Belle obtains $|\sin(2\phi_1 + \phi_3)| > 0.44(0.13)$ and $|\sin(2\phi_1 + \phi_3)| > 0.52(0.07)$ at 68% (90%) C.L. using $B \rightarrow D^*\pi$ and $B \rightarrow D\pi$, respectively. BaBar constrains $\sin(2\phi_1 + \phi_3)$ combining $B \rightarrow D^{(*)}\pi$ and $B \rightarrow D\rho$ as $|\sin(2\phi_1 + \phi_3)| > 0.64(0.40)$ at 68% (90%) C.L.

References

1. N. Cabibbo, *Phys. Rev. Lett.*, 10:531–532 (1963).
2. M. Kobayashi and T. Maskawa, *Prog. Theor. Phys.*, 49:652–657 (1973).
3. K. Abe *et al.*, *Phys. Rev. Lett.*, 87:091802 (2001).
4. B. Aubert *et al.*, *Phys. Rev. Lett.*, 87:091801 (2001).
5. A. B. Carter and A. I. Sanda, *Phys. Rev. Lett.*, 45:952 (1980).
6. A. B. Carter and A. I. Sanda, *Phys. Rev. D*, 23:1567 (1981).
7. I. I. Bigi and A. I. Sanda, *Nucl. Phys. B*, 193:85 (1981).
8. M. Gronau and D. London, *Phys. Rev. Lett.*, 65:3381–3384 (1990).
9. A. E. Snyder and H. R. Quinn, *Phys. Rev. D*, 48:2139–2144 (1993).
10. H. J. Lipkin, Y. Nir, H. R. Quinn, and A. E. Snyder, *Phys. Rev. D*, 44:1454–1460 (1991).
11. M. Gronau, *Phys. Lett. B*, 265:389–394 (1991).
12. M. Gronau and J. Zupan, *Phys. Rev. D*, 70:074031 (2004).
13. M. Gronau, E. Lunghi, and D. Wyler, *Phys. Lett. B*, 606:95–102 (2005).
14. M. Gronau and J. Zupan, *Phys. Rev. D*, 73:057502 (2006).
15. M. Beneke, M. Gronau, J. Rohrer, and M. Spranger, *Phys. Lett. B*, 638:68–73 (2006).
16. H. Ishino *et al.*, *Phys. Rev. Lett.*, 98:211801 (2007).
17. B. Aubert *et al.*, hep-ex/0703016 (2007).
18. Heavy Flavor Averaging Group (HFAG), hep-ex/0603003 (2006); and online update of Summer 2006 (<http://www.slac.stanford.edu/xorg/hfag>).
19. CKMfitter, <http://www.slac.stanford.edu/xorg/ckmfitter/>.
20. UTfit, <http://utfit.roma1.infn.it/>.
21. A. Somov, A. J. Schwartz, *et al.*, *Phys. Rev. Lett.*, 96:171801 (2006).
22. B. Aubert, arXiv:0705.2157 [hep-ex] (2007).
23. B. Aubert *et al.*, *Phys. Rev. Lett.*, 98:111801 (2007).
24. J. Zhang *et al.*, *Phys. Rev. Lett.*, 91:221801 (2003).
25. B. Aubert *et al.*, *Phys. Rev. Lett.*, 97:261801 (2006).
26. K. Abe *et al.*, hep-ex/0702009 (2007).
27. A. Kusaka, C. C. Wang, H. Ishino, *et al.*, hep-ex/0701015 (2007).
28. B. Aubert *et al.*, hep-ex/0703008 (2007).
29. B. Aubert *et al.*, hep-ex/0701035 (2007).

30. B. Aubert *et al.*, *Phys. Rev. Lett.*, 98:181803 (2007).
31. A. Giri, Y. Grossman, A. Soffer, and J. Zupan, *Phys. Rev. D*, 68:054018 (2003).
32. A. Bonder, Proceedings of BINP Special Analysis Meeting on Dalitz Analysis, 24-26 Sep. 2002, unpublished.
33. M. Gronau and D. London, *Phys. Lett. B*, 253:483–488 (1991).
34. M. Gronau and D. Wyler, *Phys. Lett. B*, 265:172–176 (1991).
35. D. Atwood, I. Dunietz, and A. Soni, *Phys. Rev. Lett.*, 78:3257–3260 (1997).
36. D. Atwood, I. Dunietz, and A. Soni, *Phys. Rev. D*, 63:036005 (2001).
37. I. Dunietz and R. G. Sachs, *Phys. Rev. D*, 37:3186–3192 (1988). *Erratum: Phys. Rev. D*, 39:3515 (1989).
38. I. Dunietz, *Phys. Lett. B*, 427:179–182 (1998).
39. A. Poluektov *et al.*, *Phys. Rev. D*, 73:112009 (2006).
40. B. Aubert *et al.*, hep-ex/0607104 (2006).
41. B. Aubert *et al.*, hep-ex/0703037 (2007).
42. K. Abe *et al.*, *Phys. Rev. D*, 73:051106 (2006).
43. B. Aubert *et al.*, *Phys. Rev. D*, 72:071103 (2005).
44. B. Aubert *et al.*, *Phys. Rev. D*, 73:051105 (2006).
45. K. Abe *et al.*, hep-ex/0508048 (2005).
46. B. Aubert *et al.*, *Phys. Rev. D*, 72:071104 (2005).
47. R. Fleischer, *Nucl. Phys. B*, 671:459–482 (2003).
48. F. J. Ronga, T. R. Sarangi, *et al.*, *Phys. Rev. D*, 73:092003 (2006).
49. B. Aubert *et al.*, *Phys. Rev. D*, 71:112003 (2005).
50. B. Aubert *et al.*, *Phys. Rev. D*, 73:111101 (2006).